Short Communication

Optimal design of absorptive glass mat (AGM) separator with fastest electrolyte uptake using X-ray micro-computed tomography

AMIT RAWAL[a,b], P.V.KAMESWARA RAO[a], VIJAY KUMAR[c], SUMIT SHARMA[a], SIDDHARTH SHUKLA[a], DÁNIEL SEBŐK[d], IMRE SZENTI[e], AKOS KUKOVECZ[e1]

[a]*Indian Institute of Technology Delhi*

Hauz Khas, New Delhi, India

[b]*Fraunhofer Institute for Industrial Mathematics (ITWM)*

Fraunhofer-Platz 1, D-67663 Kaiserslautern, Germany

[c] *ENSAIT, GEMTEX – Laboratoire de Génie et Matériaux Textiles, F-59000 Lille, France*

[d] *Department of Materials Science, University of Szeged, Rerrich Béla tér 1., Szeged, Hungary*

[e] *Department of Applied and Environmental Chemistry, University of Szeged, Rerrich Béla tér 1., Szeged, Hungary*

Abstract

Valve regulated lead acid (VRLA) batteries are traditionally classified on the basis of gel and absorptive glass mat (AGM) separators. To fulfill the desired functions of AGM batteries, a key design feature of the separator relies on the uptake of the electrolyte in shortest transport time. Herein, we present a three-dimensional (3D) analytical model to predict the fastest electrolyte uptake in AGM separators based upon the optimal set of fiber and structural parameters. The predictive model has utilized 3D data of fiber orientation in AGM separators, obtained via X-ray

[1]Corresponding Authors: Tel/Fax: +36 62 544620/ +36 62 544619. E-mail: kakos@chem.u-szeged.hu

micro-computed tomography analysis. Such realistic structural information of AGM has assisted in simulating the separators made up of cheaper coarser glass fibers, which was subsequently benchmarked with the experimental samples consisting of finer fibers for attaining the fastest electrolyte uptake. Through theoretical modeling, a design criterion has successfully evolved for the fastest electrolyte uptake by mapping the key effects of the fiber diameter, 3D fiber orientation distribution and porosity of AGM separators. In general, high-density AGM separators comprising of preferentially aligned coarser fibers tend to attain the fastest electrolyte uptake.

Keywords: fiber orientation; electrolyte uptake; separator; wicking

1. Introduction

Absorptive glass mat (AGM) batteries are amongst the widely used lead-based batteries that have gained popularity with an ever-increasing list of applications. The separator, a key component of the AGM battery, has played a pivotal role in enhancing the life cycle of the battery [1–3]. These separators are prepared using glass fibers via paper-making process and host a multitude of characteristics including separation of electrodes, maintaining good contact with the electrodes and retain electrolyte reliably [2,4–8]. The movement of the electrolyte within an AGM separator can be instigated via filling processes namely, gravity top fill, gravity bottom-up fill, push fill, soft-vacuum fill, and hard-vacuum fill [9]. Amongst these filling processes, gravity bottom-up fill is the most reproducible method in terms of fill weight, uniform distribution and saturation level [9]. This method involves imbibing the AGM separator into a bath of electrolyte solution and the movement of the electrolyte is primarily dictated by wicking. One of the major demerits of the gravity bottom-up fill method is profoundly related to the slow process of wicking [9]. Inevitably, the slow wicking of electrolyte restricts a practical limit on the battery dimensions, which

effectively limits the applications of this method to the large batteries [10]. To enhance the electrolyte uptake, a key set of fiber and structural parameters needs to be optimized in an AGM separator.

In general, the wicking characteristics of AGM separators are governed by fiber properties (diameter, length, wetting characteristics), structural parameters (porosity, pore geometry, bulk density), and compression hysteresis developed as a result of charge and discharge modes of the battery [4,11–15]. In the seminal work of Culpin [16], an attempt was made to predict the wicking characteristics of AGM separators using well-known Lucas-Washburn [17,18] equation specifically for a short time duration (~8 mins). Notably, Lucas-Washburn [17,18] equation did not account for the effect of gravity. Through semi-analytical approach, Kamenev et al. [19] proposed the model of wicking characteristics by considering the effect of gravity but the realistic structural characteristics of AGM separators did not feature into the modeling scheme. Recently, the analytical models of wicking characteristics of AGM separators have been proposed by considering key set of fiber and structural parameters based upon Fries and Dreyer approach that included the effect of gravity component [13,15,20]. Defying gravity is a major challenge to design an AGM separator for the fastest uptake of electrolyte. In the open literature, a theoretical framework to compute minimum time taken by the electrolyte solution to reach a predefined wicking height in an AGM separator has not been developed. Therefore, the central aim of the research work was to propose an analytical model to predict the optimal set of fiber and structural parameters of AGM separators for the fastest electrolyte uptake. The synergistic effect of key fiber properties and structural parameters along with the interplay of gravity, capillary pressure and viscous effects has formed the basis of the predictive model for computing the fastest electrolyte uptake in AGM separators. A parametric analysis has allowed us to redesign the AGM

separators and subsequently, a comparison was made between the hypothesized and experimentally obtained samples. In this research work, X-ray micro-computed tomography (microCT) analysis has been utilized in obtaining the 3D fiber orientation distribution of AGM separators, a key structural parameter which has been used as an input parameter in modeling the fastest electrolyte uptake.

2. Theoretical Analysis

Gravity bottom-up filling method involves the battery consisting of AGM separators to be imbibed in a bath of electrolyte to ingress the separator and electrodes with acid by means of wicking [9], as illustrated in Fig. 1. In general, AGM separators are highly porous materials that consist of a three-dimensional (3D) anisotropic network of glass fibers. The pores of AGM separators not only enable the distribution of electrolyte but also hinder the acid stratification [12,16,21,22]. To attain the fastest electrolyte uptake in the pore channels of an AGM separator, it is pertinent to understand the interplay of gravity, capillary pressure, viscous and inertia effects through momentum balance equation of a liquid inside a capillary tube, as shown below [20].

$$\frac{4\sigma\cos\zeta}{D} = \rho g h \sin\psi + \frac{\varphi_p \mu h}{K}\dot{h} + \rho\frac{d\left(h\dot{h}\right)}{dt} \tag{1}$$

where σ is the liquid surface tension, ζ is the liquid contact angle, D is the capillary diameter, ρ is the liquid density, g is the acceleration due to gravity, h is the distance covered by the liquid, μ is the dynamic viscosity, φ_p is the porosity, t is the time taken by the liquid, ψ is the inclination angle of the porous medium, and K is the permeability of porous medium.

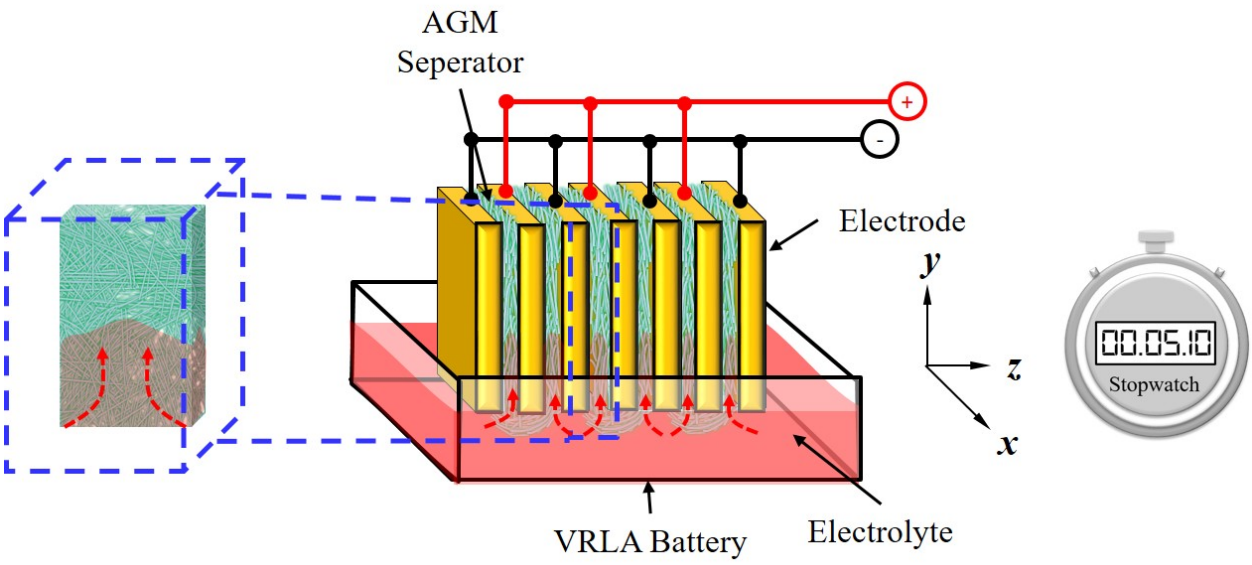

Fig.1. A schematic display of AGM separators and electrodes imbibed in an electrolyte solution. Here, the magnified view of an AGM separator illustrates the electrolyte uptake *whilst* the stopwatch depicts the transport time taken by the electrolyte solution.

Fries and Dreyer [20] successfully solved the above equation by neglecting the effect of inertia to formulate a relationship between the time (t) required for a liquid to travel a defined height (h) through a particle-based porous medium. Thus,

$$t = \frac{-h}{b} - \frac{a}{b^2}\ln\left(1 - \frac{bh}{a}\right) \tag{2}$$

where, $a = \dfrac{4\sigma K\cos\zeta}{D\varphi_p\mu}, b = \dfrac{\rho Kg\sin\psi}{\varphi_p\mu}$. (3)

For non-circular pore channels in an AGM separator, we earlier introduced the concept of hydraulic diameter (D_H) to replace the capillary diameter (D) in Eq. (3) [13]. Owing to the fact that AGM separators possess 3D anisotropy which eventually gives rise to the directional

anisotropy both in hydraulic diameter and permeability, as illustrated by Mao and Russell [23]. Thus,

$$K(\vartheta) = -\frac{d_f^2 PST}{32\left(1-\varphi_p\right)}$$
$$D_H(\vartheta) = d_f \frac{\varphi_p}{1-\varphi_p} Q \tag{4}$$

where,

$$P = \left[\frac{1}{\int_0^{\pi} d\phi \int_0^{\pi} \left\{ T\cos^2\chi + S\sin^2\chi \right\} \Omega(\theta,\phi)\sin\theta d\theta} \right],\ S = -\left[4\left(1-\varphi_p\right) - \left(1-\varphi_p\right)^2 - 3 - 2\ln\left(1-\varphi_p\right) \right],$$

$$T = \ln\left(1-\varphi_p\right) + \frac{1-\left(1-\varphi_p\right)^2}{1+\left(1-\varphi_p\right)^2}$$

$$Q = \frac{1}{\int_0^{\pi} d\phi \int_0^{\pi} \Omega(\theta,\phi)\left|\cos\chi\right|\sin\theta d\theta},\ \cos\chi = \cos\theta\cos\theta_f + \sin\theta\sin\theta_f\cos\left(\phi-\phi_f\right) \tag{5}$$

where d_f is the fiber diameter, χ is the angle formed between the alignment of AGM sample and the direction of liquid flow $\left(\theta_f, \phi_f\right)$, $\Omega(\theta,\phi)$ is the fiber orientation distribution function, θ and ϕ are the polar and azimuthal orientation angles, respectively.

It should be noted that the flow of the electrolyte takes place primarily in the machine (in-plane) direction resulting in $\theta_f = \frac{\pi}{2}$, $\phi_f = 0$ and $\cos\chi = \sin\theta\cos(\phi)$, using Eq. (5). Nevertheless, based upon the above considerations, the parameters *a* and *b* given in Eq. (3) can be rewritten as [13],

$$a=\frac{4\sigma K\left(\vartheta\right)\cos\zeta}{D_H\left(\vartheta\right)\varphi_p\mu},\ b=\frac{\rho K\left(\vartheta\right)g\sin\psi}{\varphi_p\mu} \tag{6}$$

Combining Eqs. (2)-(4) and (6) yields the following expression,

$$t=-\frac{E}{D_H^2\left(\vartheta\right)}-\frac{B}{D_H^3\left(\vartheta\right)}\ln\left(1-FD_H\left(\vartheta\right)\right) \tag{7}$$

where, $F=\frac{\rho gh\left(t\right)\sin\psi}{4\sigma\cos\zeta}$, $B=\frac{128\sigma\cos\zeta Q^2\mu\varphi_p^3}{\rho^2g^2\sin^2\psi(\varphi_p-1)PST}$, $E=-\frac{32Q^2\varphi_p^3\mu h(t)}{\rho g\sin\psi\left(1-\varphi_p\right)PST}$

In order to find the hydraulic diameter, $D_H\left(\vartheta\right)$ that can lead to the fastest electrolyte uptake, Eq. (7) needs to be differentiated with respect to $D_H\left(\vartheta\right)$ and also satisfying the following condition.

$$\frac{dt}{dD_H\left(\vartheta\right)}=0\Rightarrow\frac{3B\ln(1-FD_H\left(\vartheta\right))}{D_H\left(\vartheta\right)}+\frac{BF}{1-FD_H\left(\vartheta\right)}+2E=0 \tag{8}$$

The solution of the Eq. (8) yields the magnitude of hydraulic diameter, $D_H\left(\vartheta\right)$ or capillary dimensions, which takes minimum time by the electrolyte to reach the defined height (*h*) in an AGM separator. However, the condition, i.e. $\frac{d^2t}{dD_H^2\left(\vartheta\right)}>0$ is required to be satisfied, or,

$$\frac{d^2t}{dD_H^2\left(\vartheta\right)}=\frac{-6D_H\left(\vartheta\right)\left(1-FD_H\left(\vartheta\right)\right)^2E-12B\left(1-FD_H\left(\vartheta\right)\right)^2\ln\left(1-FD_H\left(\vartheta\right)\right)-BFD_H\left(\vartheta\right)(6-7FD_H\left(\vartheta\right))}{D_H^5\left(\vartheta\right)\left(1-FD_H\left(\vartheta\right)\right)^2}>0 \tag{9}$$

It should be noted that Eq. (8) cannot have real roots if $FD_H\geq1$, and for porous materials such as AGM separators $D_H>0$, or in other words, $0\leq FD_H<1$, hence $D_H^5\left(1-FD_H\right)^2>0$ in Eq. (9). Further, $\frac{d^2t}{dD_H^2\left(\vartheta\right)}>0$ if the following condition is satisfied,

$$-6D_H\left(1-FD_H\right)^2 E-12B\left(1-FD_H\right)^2 \ln\left(1-FD_H\right)-BFD_H(6-7FD_H)>0 \qquad (10)$$

Satisfying the Eq. (10) would inevitably result in the magnitude of $D_H\left(\vartheta\right)$, which would yield the minimum wicking time taken by the electrolyte to reach the defined height. Moreover, $D_H\left(\vartheta\right)$ is dependent upon the fiber and structural parameters of AGM namely, porosity, fiber diameter and alignment of fibers within an AGM separator, as shown in Eq. (4). Accordingly, various combinations of the magnitudes of these input parameters have been used to obtain the values of $D_H\left(\vartheta\right)$ that matches with those obtained from Eq. (8).

3. Experimental Work

The proposed model of fastest electrolyte uptake was evaluated using two AGM samples namely 'A' and 'B'. Here, the sample 'B' is identified as the same sample that was used in our previous publications [14,15]. A key set of fiber and AGM properties was determined, as highlighted in Table 1. Specifically, the images obtained from the scanning electron microscope (ZEISSEVO 50) were used concomitantly with IMAGEJ® software for computing the fiber diameter in AGM samples. Moreover, the wicking tests for both AGM samples were specifically performed in a confined state, using the approach given in references [13,15]. Here, the wicking height was measured by placing the AGM specimen of dimensions, i.e., 32 mm x 1200 mm in the machine (production) direction. The movement of the battery grade electrolyte solution (density = 1.28 g cm^{-3}, 4.93 M) tinted with methyl orange color was detected in intervals of 5 mm. The confined state of AGM separator was attained by sandwiching the specimen between the acrylic plates, which was subsequently compressed up to 20% of the initial thickness. Further details of the

wicking tests are given in references [13,15]. An average of three repeated readings was considered for determining the wicking height of AGM separators.

Table 1 Characteristics of AGM separators and constituent fibers

Parameter	Units	Sample ID	
		A	B
Mass per unit area	gm^{-2}	297±5.4	303±4.6 [13]
Initial thickness	mm	2.12±0.07	2.59±0.07 [13]
Fiber volume fraction	-	0.10	0.08
MD[$]/CD[#] ratio of tensile strength	-	1.56	1.52
Fiber diameter	µm	1.31±0.87	1.46±0.1.27 [13]
Fiber density	gcm^{-3}	2.45 [13]	

[$]MD: Machine direction

[#]CD: Cross-machine direction

3D fiber orientation distribution of sample A was obtained via X-ray micro-computed tomography analysis, which was conducted using the X-ray Microtomography equipment (SkyScan 2211). The sample dimensions of 2.25 x 2.2 x 2 mm^3 were scanned using 11Mp cooled CCD camera by applying the source voltage of 50 kV and source current of 600 µA with an exposure time of 600 ms. 1292 projection images were obtained for 180^o in a scan time of 72 min by employing a rotation step of 0.15^o. NRecon Reconstruction Software, and CtVox software (Skyscan, Bruker, Belgium) were then used to reconstruct the projected images with a pixel size of 4032 x 2688. Subsequently, 240554 readings of 3D fiber orientation angles were obtained using CTAn (CT Analyser) software. A typical representative volume rendered 3D image of sample A is depicted

in Fig. 2. For sample B, 3D fiber orientation distribution was obtained via X-ray micro-computed tomography analysis, which was previously determined in the reference [14].

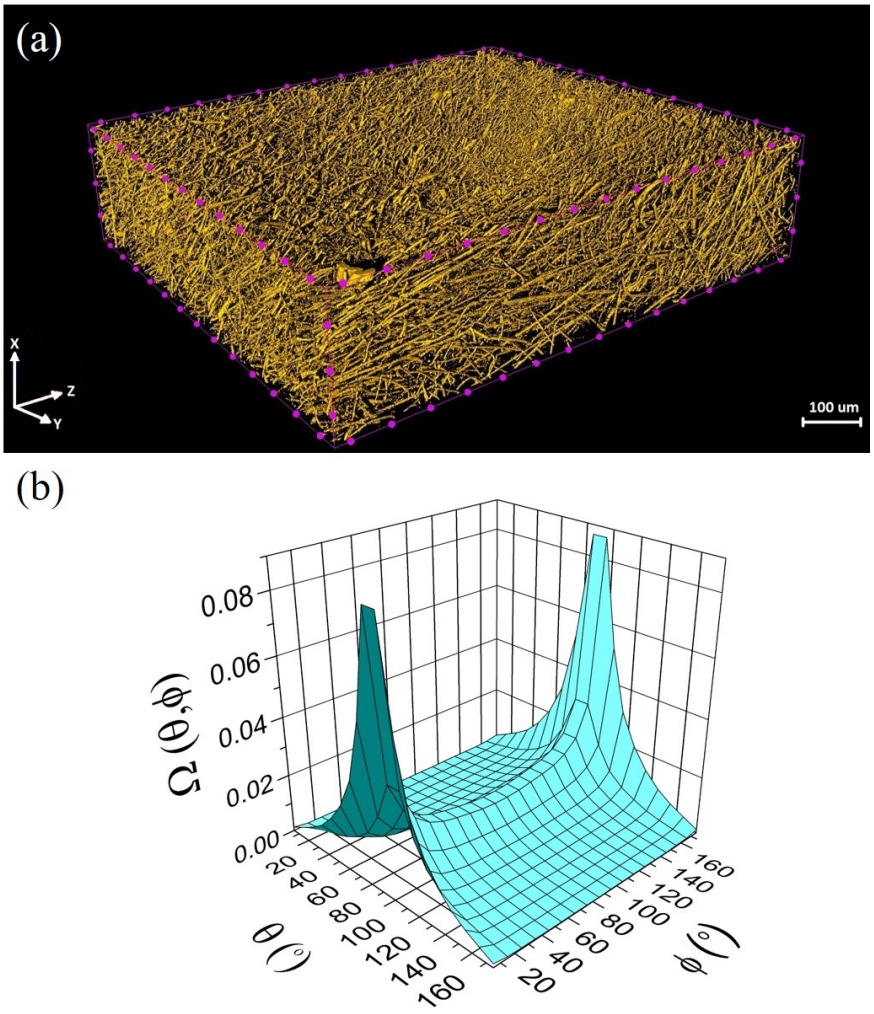

Fig. 2. (a) 3D rendered image and (b) 3D fiber orientation distribution of sample A obtained via X-ray microCT analysis. Here, $\Omega(\theta,\phi)$ is the fiber orientation distribution function whereas, θ and ϕ are the polar (out-of-plane) and azimuthal (in-plane) orientation angles, respectively. Here, 0^o and 90^o represent the machine and planar directions in the in-plane and out-of-plane fiber orientation distributions, respectively.

4. Results and discussion

AGM consists of an interconnected 3D network of fibers, which forms intricate pore geometry in terms of varying shapes and sizes [12]. Such a complex 3D porous structure forms a tortuous path for the movement of the electrolyte within an AGM separator. The synergy between the porous structure of AGM separator, constituent fiber dimensions and level of compression forces within the battery play a vital role in mediating the electrolyte uptake [11–13,19,24]. Given the fact that the fiber alignment within an AGM separator dictates the 3D pore geometry [15], it is imperative to determine the 3D fiber orientation distribution [21]. With the aid of the microCT analysis, the 3D fiber orientation distribution of AGM separators has been successfully obtained and analyzed. Fig. 2b shows the 3D fiber orientation distribution of sample A. As expected, it can be clearly seen that the in-plane fibers are preferentially aligned in the machine (production) direction. This observation corroborates well with the ratio of tensile strength in the machine direction (MD) to the cross-machine direction (CD) of both samples, which reveals the anisotropic characteristics (see Table 1). On the other hand, a majority of the out-of-plane fibers are aligned in the in-plane direction ($\theta = 90^o$) but there is a certain proportion of fibers, which are aligned in various out-of-plane directions that affect the flow of the electrolyte, and therefore, were accounted in the modeling scheme. Nevertheless, the preferential alignment of the in-plane fibers assists in transporting the electrolyte at a higher wicking rate corresponding to randomly aligned fibers in AGM separators [13,25]. Accordingly, the predictive ability of the proposed analytical model was assessed by computing the wicking time to attain the desired height in the machine (preferential) direction. Fig. 3 shows a comparison of wicking time to attain a height of 20 cm by hypothesized AGM separators and experimental samples. Here, the hypothesized AGM separators consist of the same structural characteristics (porosity, 3D fiber orientation distribution) as that of the

experimental samples. However, the constituent fiber diameter is significantly different in hypothesized and experimental AGM samples.

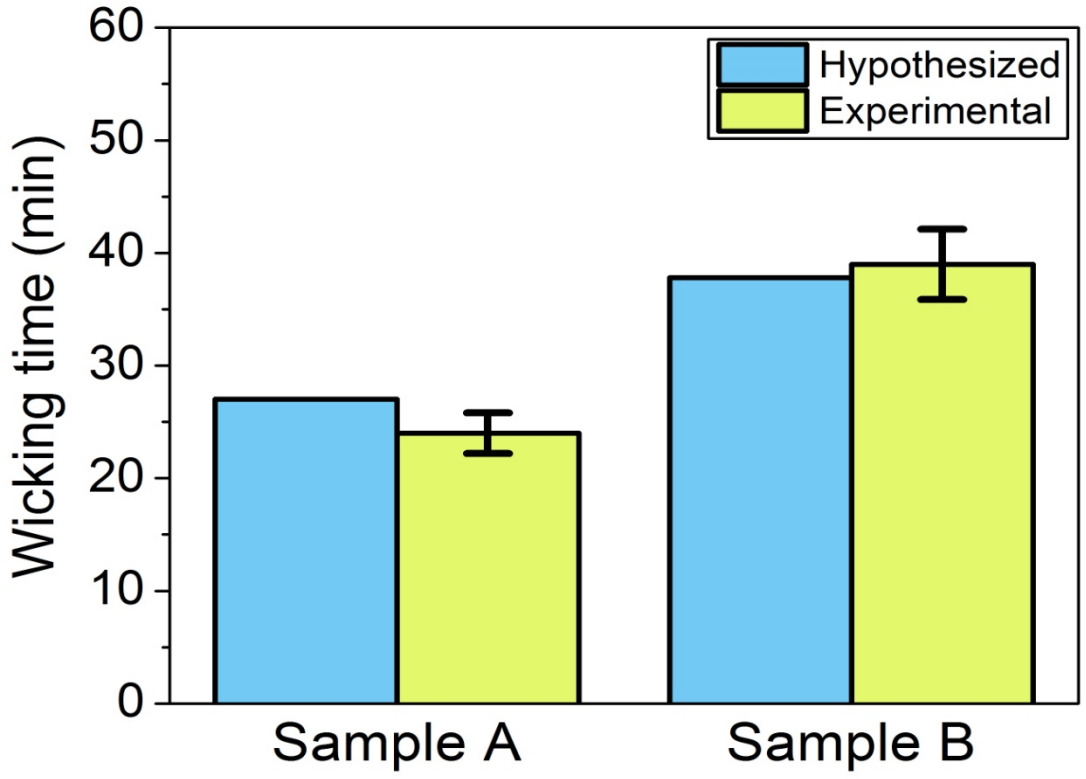

Fig.3. Comparison of time taken by the electrolyte solution in hypothesized and experimental AGM samples to reach a predefined wicking height (~20 cm).

Ideally, the hypothesized samples A and B consist of fibers having diameters of 5.1 and 3.7 μm, respectively; whereas the experimental samples possessed a large variation in fiber diameter (see Table 1 and Fig. S1). This clearly shows that the coarser fibers could easily replace finer fibers for attaining the wicking height of 20 cm in the same time duration. For batteries with low height to plate spacing ratio (<50), the replacement of finer fibers with coarser entities would not only save the cost but the latter can act as a 'pump' leading to higher wicking rates [26,27]. Although, the merits of finer fibers cannot be ignored as these fibers promote the electrolyte solution to

greater wicking heights at a fast rate without allowing electrolyte drainage and inhibit acid stratification in addition to the improvement in the mechanical stability [26,27]. Nevertheless, the design of an AGM separator can be tailored for a defined application by considering the plate height to plate spacing ratio.

From the structural point of view, the porosity of AGM separator is a well-known parameter that modulates the wicking characteristics [7,12]. For instance, an AGM separator with a higher porosity is anticipated to yield a higher saturation level than a lower porosity separator [12]. However, the time taken by the electrolyte movement in an AGM separator depends upon the local pore shapes and dimensions [7], which is further dependent upon the overall porosity, fiber dimensions and alignment of fibers within the separator [13]. To look at this issue profoundly, a virtual experiment was conducted to map the effects of the fiber diameter, fiber orientation distribution and the porosity of AGM separators to attain predefined wicking height in shortest transport time, as shown in Fig. 4. Here, the effect of three distinct fiber orientation distributions was analyzed on the fastest wicking time and is depicted in Fig. S2 (see supplementary information). Intriguingly, preferentially aligned coarser fibers in high-density AGM separators have attained the fastest wicking time. Ostensibly, greater in-plane fiber alignment and AGM density promote fibers to act as capillaries for the transportation of the electrolyte because the glass fibers exhibit zero contact angle with the electrolyte solution [5]. Further, the coarser fibers allow the formation of larger channels or pores with smaller frictional resistance that enables easier access by the electrolyte [28]. It is worth mentioning that the condition, i.e., $\frac{d^2t}{dD_H^2(\vartheta)} > 0$ has always been satisfied in all the proposed cases (see Table S1).

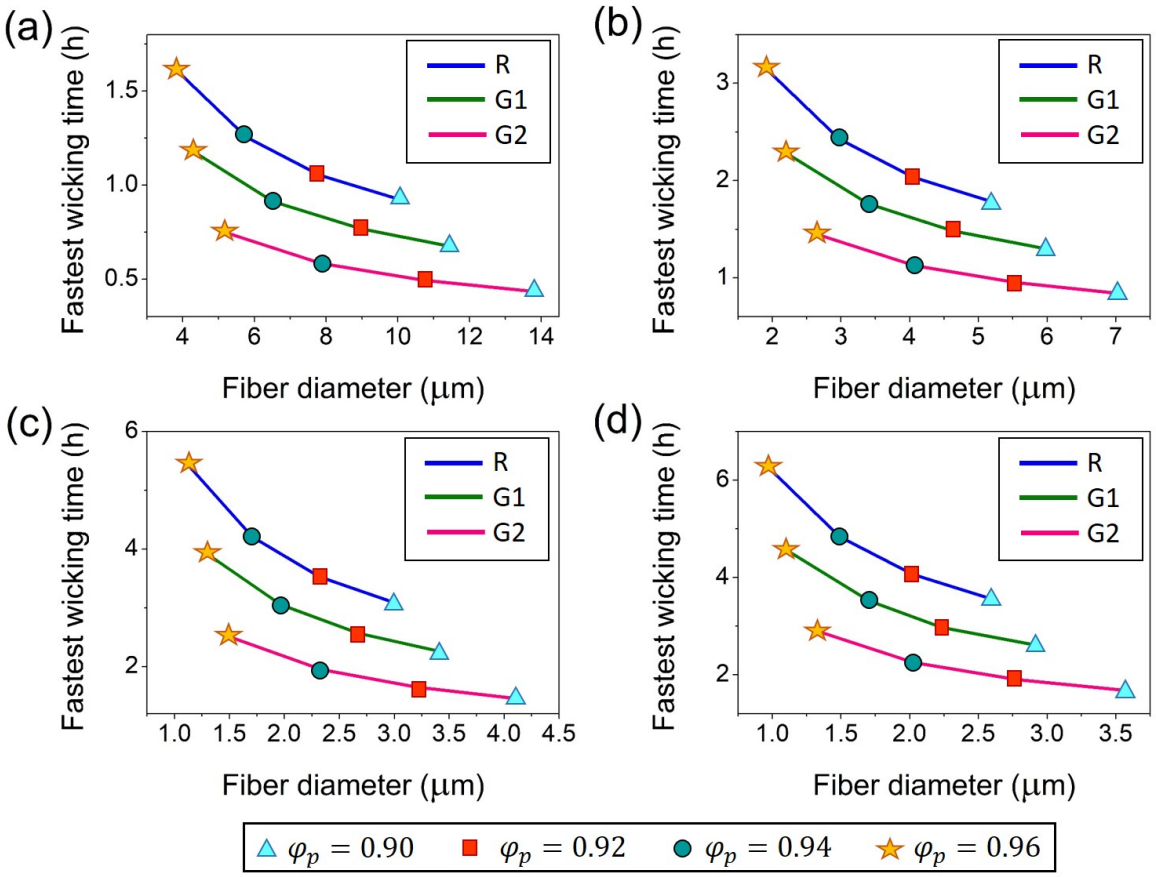

Fig. 4. Fastest wicking time as a function of fiber diameter, fiber orientation distribution and porosity of AGM separator, which is vertically aligned ($\psi = 90^0$) to attain a wicking height of (a) 40 cm (b) 60 cm (c) 80 cm and (d) 100 cm. Here, the in-plane fiber orientation distribution is represented by random (R) distribution, and G1 and G2 are represented by Gaussian distributions having mean of 90° and standard deviations of 50° and 30°, respectively, whereas out-of-plane fiber orientation distribution is considered to be random in nature.

In general, the presented results support the rationale of using AGM separator of higher density for the improvement in the life cycle of the battery. Since, the magnitude of the compressive stresses experienced by the electrodes both in the dry and wet states is also anticipated to be the same along with minimum compression hysteresis [6,7,14].

5. Conclusions

In this research work, a 3D analytical model to predict the fastest electrolyte uptake in AGM separators has been proposed on the basis of the optimal set of key fiber and structural parameters along with the interplay of gravity, capillary pressure and viscous effects. The X-ray microCT analysis has been applied to obtain the 3D fiber orientation distribution, which was used as a key input parameter in the predictive model. Based upon the realistic structural information of experimental samples, the proposed model has successfully benchmarked hypothesized AGM separators made up of cheaper coarser fibers with those of experimental samples consisting of finer fibers to attain the fastest electrolyte uptake for a predefined wicking height (~20 cm). The key effects of the fiber diameter, 3D fiber orientation distribution and porosity of AGM separators were mapped to attain predefined wicking height in shortest transport time. Theoretically, the high-density AGM separators with preferentially aligned coarser fibers have attained the fastest electrolyte uptake. Future studies should focus on the development of a predictive model of fastest electrolyte uptake in the multi-component AGM separator comprising of a defined proportion of constituent glass fibers or a blend of glass and other types of fibers.

Acknowledgment

This work has been financially supported by Indo-Hungarian joint research project no. INT/HUN/P-18/2017. IS and AK acknowledge the financial support from the "Széchenyi 2020" program in the framework of GINOP-2.3.2-15-2016-00013 project and the NKFIH K 126065 grant. DS thanks the Hungarian Academy of Sciences for a János Bólyai Postdoctoral Research Fellowship.

References

[1] M. Krishna, E.J. Fraser, R.G.A. Wills, F.C. Walsh, Developments in soluble lead flow batteries and remaining challenges: An illustrated review, J. Energy Storage. 15 (2018) 69–90.
[2] Y. Nakayama, K. Kishimoto, S. Sugiyama, S. Sakaguchi, Micro-structural design and function of an improved absorptive glass mat (AGM) separator for valve-regulated lead–acid batteries, J. Power Sources. 107 (2002) 192–200.
[3] M.J. Weighall, Keeping up the pressure—strategies to maintain plate-group pressure and extend the cycle life of VRLA batteries, J. Power Sources. 95 (2001) 209–217.
[4] G.C. Zguris, Fluid-transfer properties of recombinant battery separator media, J. Power Sources. 88 (2000) 36–43.
[5] G.C. Zguris, A review of physical properties of separators for valve-regulated lead/acid batteries, J. Power Sources. 59 (1996) 131–135.
[6] G.C. Zguris, Advances in recombinant battery separator mat (RBSM) separators for lead-acid batteries—a review, J. Power Sources. 107 (2002) 187–191.
[7] G.C. Zguris, 'Density/solidity'of recombinant battery separator material—its influence on both separator and battery performance in valve-regulated lead- acid systems, J. Power Sources. 133 (2004) 67–78.
[8] G.C. Zguris, Absorptive glass-mat separators for valve-regulated lead/acid batteries—thoughts on compression, J. Power Sources. 67 (1997) 307–313.
[9] M.J. Weighall, Techniques for jar formation of valve-regulated lead–acid batteries, J. Power Sources. 116 (2003) 219–231.
[10] G.J. May, A. Davidson, B. Monahov, Lead batteries for utility energy storage: A review, J. Energy Storage. 15 (2018) 145–157.
[11] K. McGregor, A.F. Hollenkamp, M. Barber, T.D. Huynh, H. Ozgun, C.G. Phyland, A.J. Urban, D.G. Vella, L.H. Vu, Effects of compression on recombinant battery separator mats in valve-regulated lead–acid batteries, J. Power Sources. 73 (1998) 65–73.
[12] K. McGregor, H. Ozgun, A.J. Urban, G.C. Zguris, Essential characteristics for separators in valve-regulated lead–acid batteries, J. Power Sources. 111 (2002) 288–303.
[13] V. Kumar, P.K. Rao, A. Rawal, Amplification of electrolyte uptake in the absorptive glass mat (AGM) separator for valve regulated lead acid (VRLA) batteries, J. Power Sources. 341 (2017) 19–26.
[14] P.K. Rao, A. Rawal, V. Kumar, K.G. Rajput, Compression-recovery model of absorptive glass mat (AGM) separator guided by X-ray micro-computed tomography analysis, J. Power Sources. 365 (2017) 389–398.
[15] A. Rawal, P.K. Rao, V. Kumar, Deconstructing three-dimensional (3D) structure of absorptive glass mat (AGM) separator to tailor pore dimensions and amplify electrolyte uptake, J. Power Sources. 384 (2018) 417–425.
[16] B. Culpin, Separator design for valve-regulated lead/acid batteries, J. Power Sources. 53 (1995) 127–135.
[17] R. Lucas, Rate of capillary ascension of liquids, Kolloid Z. 23 (1918) 15–22.
[18] E.W. Washburn, The dynamics of capillary flow, Phys. Rev. 17 (1921) 273.
[19] Y. Kamenev, M. Lushina, E. Ostapenko, Investigation of the height and rate of capillary lift of electrolyte in the glass-mat separator of a sealed lead-acid battery, J. Power Sources. 109 (2002) 276–280.
[20] N. Fries, M. Dreyer, An analytic solution of capillary rise restrained by gravity, J. Colloid Interface Sci. 320 (2008) 259–263.

[21] B. Culpin, K. Peters, Saturation influences on the performance of valve-regulated lead–acid batteries, J. Power Sources. 144 (2005) 313–321.
[22] V. Toniazzo, Amersorb: a new high-performance polymeric separator for lead–acid batteries, J. Power Sources. 144 (2005) 365–372.
[23] N. Mao, S.J. Russell, Capillary pressure and liquid wicking in three-dimensional nonwoven materials, J. Appl. Phys. 104 (2008) 034911.
[24] R.V. Biagetti, I.C. Baeringer, F.J. Chiacchio, A.G. Cannone, J.J. Kelley, J.B. Ockerman, A.J. Salkind, Influence of compression on microfiber glass separator and effect of orientation on battery performance, in: Telecommun. Energy Conf., 1994: pp. 39–46.
[25] R.J. Ball, R. Evans, R. Stevens, Characterisation of separator papers for use in valve regulated lead/acid batteries, J. Power Sources. 104 (2002) 208–220.
[26] V. Toniazzo, U. Lambert, Developments in absorptive glass mat separators for cycling applications and 36 V lead- acid batteries, J. Power Sources. 133 (2004) 94–103.
[27] A.L. Ferreira, A multi-layered approach for absorptive glass-mat separators, J. Power Sources. 78 (1999) 41–45.
[28] W.B. Palmer, The advance of a liquid front along a glass yarn, J. Text. Inst. Trans. 44 (1953) T391–T400.